Metallography, Microstructure, and Analysis (2020) 9:476–483
https://doi.org/10.1007/s13632-020-00656-z

Evolution of the Microstructure of Intermetallic Compounds Formed on Mild Steel During Hot Dipping in Molten Aluminum Alloy Baths

Meriem Kab[1] · Sabrina Mendil[2] · Kamel Taibi[1]

Received: 9 December 2019 / Revised: 30 April 2020 / Accepted: 22 May 2020 / Published online: 16 June 2020

Abstract

Hot-dip aluminum coating technique has been applied to improve the high-temperature oxidation resistance of steels. This method is adopted widely due to the low cost and good performance. The purpose of this paper is to study the formation of intermetallic layers during the hot dipping of mild steel into a molten aluminum bath. Mild steel specimens were immersed into molten aluminum alloy baths at 750 °C for 1 h, 2 h and 3 h. Intermetallic compounds were analyzed by optical microscope, scanning electron microscope coupled with energy-dispersive spectroscopy and X-ray diffraction analysis. This study was completed by microhardness testing. The results showed that the hot-dip aluminized layer was divided into an outer pure aluminum or aluminum–silicon topcoat and an intermetallic layer. In the bath of pure aluminum, the intermetallic layer was the thickest and consisted of an outer $FeAl_3$ layer and an inner Fe_2Al_5 layer adjacent to the steel substrate with tongue-/finger-like morphology, while in the Al–Si alloy bath, the thickness of the intermetallic layer decreased substantially and the interface intermetallic/steel substrate becomes flat. The ternary phases Al_8Fe_2Si and $Fe_3Al_2Si_3$ are identified in addition to $FeAl_3$ and Fe_2Al_5. The microhardness testing recorded high values of the intermetallic layers, up to $800Hv_{01}$, which confirms the high brittleness of the intermetallic compounds.

Keywords Hot-dip aluminizing · Fe–Al intermetallic · Fe–Al–Si intermetallic · Diffusion · SEM · EDS

Introduction

Mild steel or low carbon steel is the most commonly used as structural materials for its relatively lower cost than alloy steel. Despite this, this material cannot provide sufficient oxidation resistance at high temperatures [1, 2]. Several methods can be used for producing heat and oxidation-resistant coating on the mild steel. One of these methods consists of aluminum coatings. Hot-dip aluminizing is an effective surface coating technique to produce an aluminum coating layer over the steel surface by generating a thin and dense layer of alumina Al_2O_3 [3–8]. This process is widely used in industry for its efficiency and low cost [9–11]. It offers the advantage of improved weldability and exhibits an increased oxidation resistance at elevated temperatures [5].

The hot-dip aluminizing process is done by immersing a solid steel substrate in a bath of liquid aluminum for a period of time at a fixed temperature to form aluminide layers on the surface of the steel by the inter-diffusion phenomenon of iron and aluminum atoms. Then, the residual aluminum liquid on the surface will form an aluminum top coat layer with the same composition as the aluminum bath after removing the steel from the latter. As a result of the steel/aluminum interdiffusion, the aluminide coating possesses an outer aluminum topcoat and inner intermetallic layer at the interface between the steel substrate and the Al coating. The formation of these intermetallics is strongly influenced by the chemical composition of the Al bath, coating thickness, immersion time and the aluminizing temperature [12].

The microstructure of the intermetallic layer of mild steel dipped in pure aluminum is composed of minor $FeAl_3$ and major Fe_2Al_5, and the interface between FeAl intermetallic layer and the steel substrate is irregular and possesses

✉ Meriem Kab
meriemkab22@hotmail.fr

[1] Laboratory of Science and Materials Engineering, Department of Materials Science, Faculty of Mechanical and Process Engineering, University of Science and Technology Houari Boumediene (USTHB), BP32, 16111 El Alia, Bab Ezzouar, Algiers, Algeria

[2] Department of Mechanical Engineering, Faculty of Construction Engineering, University Mouloud Mammeri of Tizi-Ouzou (UMMTO), 15100 Tizi Ouzou, Algeria

a tongue-like morphology [13]. In addition to these two phases in some works was mentioned the presence of the Fe_3Al phase at the interface steel/intermetallic [14–16]. However, these intermetallics are quite brittle which limits the formability of hot-dip aluminized parts and the irregular interface acts as a stress concentrator on the aluminide layer. The intermetallic layer with a rough interface can easily crack as a flat interface when external loads are applied to the aluminized steel during assembly procedures at room temperature [14]. Therefore, in industry, silicon is frequently used in the aluminum bath to reduce the thickness of the brittle intermetallic layer [17]. Study concerning the effect of silicon on the formation of intermetallic phases in mild steel [18], indicates that adding 5 wt.% of silicon to the aluminum bath will considerably decrease the thickness of the intermetallic layer by about 85% from that of hot dipping in pure aluminum. Although the thickness of the intermetallic layer keeps reducing as the silicon content in the aluminum bath increases and the rough interface intermetallic layer/steel substrate transforms into a smooth interface. Previous studies about hot dipping in aluminum bath with various silicon content [12, 19] have proposed that the addition of 10 wt.% silicon is sufficient to reduce the thickness of the intermetallic layer and flatten the intermetallic layer/steel substrate interface. Also, the addition of silicon to the aluminum bath not only modifies the microstructure of the aluminide layer but also results in the formation of ternary Fe–Al–Si intermetallic compounds additional to FeAl intermetallic compounds [12].

The present work aims to investigate the interaction between mild steel and molten aluminum at 750 °C for various immersion times and study the effect of addition silicon in the aluminum bath during the hot-dip aluminizing process on the formation and phase identification of intermetallic layers at the interface. The mechanical properties of the reaction layers are also evaluated by microhardness indentations.

Experimental Procedures

Mild steel is used as a substrate in this study, and a commercial aluminum and aluminum–silicon alloy (AS10) are used for the aluminizing process. The chemical compositions of the adopted steel and the aluminum alloys are indicated in Table 1. In addition to the elements mentioned in the table, the Al contains traces of Bi, Ca, Co, Ga, Pb and Zr less than 1% and AS10 contains Mg, Pb and Co less than 0.6%. These elements in minimal amount do not react in the formation of intermetallics.

Aluminum baths are prepared by melting Al and Al–Si alloy in a graphite crucible containing liquid bath during the immersion of the steel. Before immersion, specimens for the hot-dip treatment were degreased in NaOH at 50 °C for 5 min, then rinsed with distilled water and pretreated in KCl at 92 °C for 2 min. The aluminizing process was carried out by immersing the steels in molten aluminum and Al–Si alloy at 750 °C for 1 h, 2 h and 3 h and then cooled down to room temperature. After hot dipping, aluminized steel specimens were prepared for cross-sectional metallographic examinations using standard grinding and polishing.

The microstructures characterization was carried out using an optical microscope and JEOL JSM 6360 scanning electron microscope coupled with an energy-dispersive (EDS) equipment. Phase identification was performed by XRD in a PANalytical X'Pert PRO diffractometer. Microhardness measurement (Hv_{01}) was taken at the surface of the coating to the steel substrate. A load of 987.7 mN was applied to the specimen for 10 s to determine the microhardness profile.

Results and Discussion

Microstructure and Phase Identification in Aluminide Layers

Hot Dipping in Al Melt

Optical micrographs of mild steel after hot dipping in Al bath at 750 °C for 1, 2 and 3 h, respectively, are shown in Fig. 1. All the aluminide layers were composed of an outer aluminum coating in the surface and an inner intermetallic layer. The steel substrate has a pearlitic–ferritic microstructure. The interface between the intermetallic layer and steel substrate has a typical morphology, which is called "tongue/finger"-like morphology in the literature [13–20], and it is oriented perpendicular to the steel substrate. We notice that after the process of hot dipping, the coating has a high roughness and the thickness was not uniform on the whole steel substrate.

It can be seen that the thickness of the intermetallic layer increases with dipping time for all specimens. The total

Table 1 Chemical composition of steel and aluminum alloys (wt.%)

Alloy	Fe	Al	Si	C	Cu	Cr	Mn	Mo	Ni	Zn	Sn	Ti
Steel	Bal.	0.008	0.24	0.24	0.25	0.15	0.6	0.04	0.16	0.001	0.01	0.01
Al	0.58	Bal.	0.26	–	0.28	0.14	0.59	–	0.12	0.22	0.11	0.08
AS10	≤0.65	Bal.	9 to 10.5	–	≤0.10	–	0.25 to 0.5	–	≤0.05	≤0.10	≤0.05	≤0.1

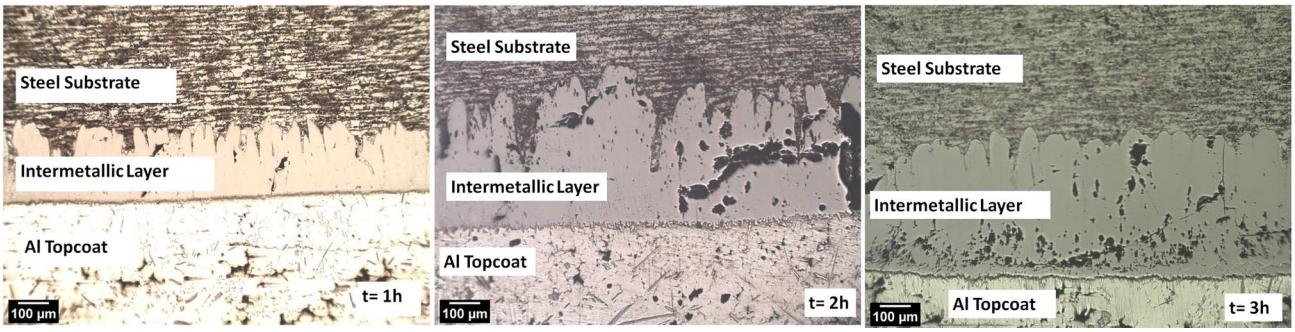

Fig. 1 Optical cross-sectional micrographs of mild steel after hot dipping into Al bath at 750 °C at different immersion times ($t = 1$ h, 2 h and 3 h)

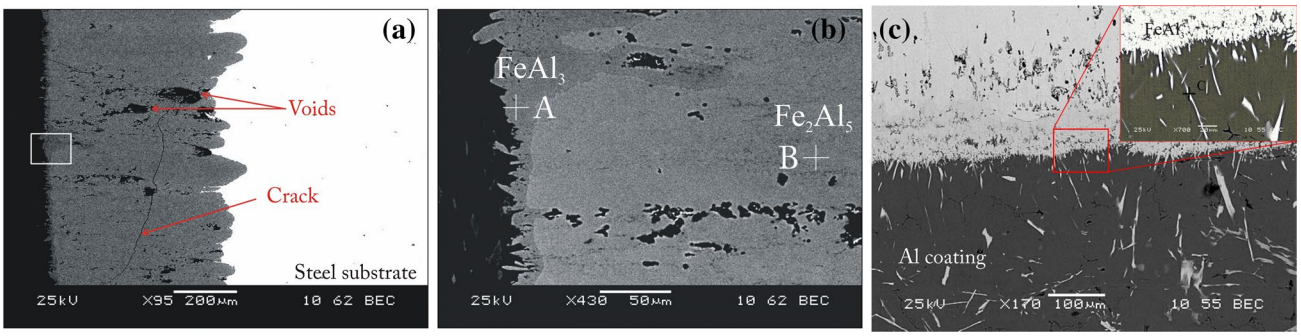

Fig. 2 (**a**) Cross-sectional BSE micrograph of intermetallic layers in mild steel after hot dipping in AL bath at 750 °C for 3 h, (**b**) BSE micrograph corresponding to the rectangular region in (**a**) and (**c**) micrograph of the outer aluminum topcoat of mild steel after hot dipping in Al bath at 750 °C for 3 h

thickness of the intermetallic layer was about 367.22 µm, 467.07 µm and 595.60 µm for an immersion time of 1, 2 and 3 h, respectively. The measurement was taken by taking the average of several measurements because of the irregularity of the morphology of the intermetallic layer.

The cross-sectional BSE micrographs of aluminized steel after dipping in Al bath at 750 °C for 3 h are shown in Fig. 2a. The aluminide layer was composed of an outer aluminum topcoat and an inner continuous Fe–Al intermetallic layer. The interface Fe–Al/steel substrate showed a tongue-like morphology, which was rougher than the interface aluminum topcoat/Fe–Al intermetallic. From the micrograph in Fig. 2b, the intermetallic layer near the aluminum topcoat displays an atomic number contrast image which possesses a thin gray outer layer about 18.38 µm in thickness and a major light gray inner layer about 570.83 µm, implying that the gray outer layer possesses a relatively lower iron content than the major light gray inner layer. The corresponding chemical compositional results determined by EDS are shown in Table 2. Referring to the Fe–Al binary phase diagram [21], this indicates that the gray outer layer near the coating which contains about 21.19% of iron and 77.94% of aluminum (point A) corresponds to the composition of $FeAl_3$

Table 2 Average composition of intermetallic phases in the aluminide layer on mild steel hot dipped into a molten aluminum bath for 3 h at 750 °C (at.%)

Position	AL K	Fe K	Mn K	Phase
A	77.94	21.19	00.87	$FeAl_3$
B	73.66	26.01	00.34	Fe_2Al_5
C	84.92	12.64	02.43	

and the inner layer adjacent to the steel substrate with the content of 26.01% of iron and 73.66% of aluminum (point B) corresponds to the composition of Fe_2Al_5. According to the EDS analysis, Mn is also present in the intermetallic layer at a very small amount, which may come from the steel substrate and the Al bath.

In the aluminum topcoat (Fig. 2c), there are dispersive compounds which possess needle-like and plate-shaped morphologies with contrast similar to that of the intermetallic layer formed following the interdiffusion of the two elements iron and aluminum. The composition of the dispersive compounds located in the aluminum topcoat is about 84.92% Al and 12.64% Fe. The high aluminum content could be

attributed to the small area of the compounds, such that the electron beam of SEM hit both the dispersive intermetallic compounds and the aluminum topcoat during EDS analysis. These compounds are formed by eutectic reaction during solidification of the Al melt and due to the dissolution of iron in the liquid Al [13].

Cracks are visible in the intermetallic layer and can be attributed to the polishing and the fragility of the intermetallic compounds. Some voids are detected at the interface between the steel and the Al coating. These voids are formed as a result of the difference mobility of Al and Fe atoms corresponding to the Kirkendall's effect [22].

The Fe_2Al_5 layer is larger than the $FeAl_3$ one, and the interface between the steel and Fe_2Al_5 appears highly irregular with peaks oriented toward the steel substrate (tongue-like morphology).

The growing of the aluminide layer was dominated by iron diffusion into a molten aluminum bath. The reaction between the solid steel and liquid Al started with the dissolution of Fe which has a higher diffusion rate in liquid than that in solid and due to the solubility of Fe in liquid Al [21], resulting, primarily, in the formation of $FeAl_3$ phase at the liquid/solid interface, followed by the formation of Fe_2Al_5 phase between $FeAl_3$ and steel substrate [23].

The growth mechanism of the Fe_2Al_5 layer is due to the 30% vacancy rate in the C-axis, [001] direction of the crystal structure of Fe_2Al_5 causing aluminum atoms to diffuse much faster inward the steel. Thus, Fe_2Al_5 tends to be oriented by the fixed C-axis of the crystal structure and grows rapidly along the diffusion direction during hot dipping causing the tongue-like morphology [20].

Hot Dipping in Al–Si Melt

Optical micrographs of mild steel after hot dipping in Al–Si bath at 750 °C for 1, 2 and 3 h, respectively, are shown in Fig. 3. The aluminide layers were composed of an outer aluminum–silicon coating on the surface and an inner intermetallic layer. The morphology of the interface intermetallic layer/steel substrate becomes smoother with the addition of silicon in the bath. The total thickness of the intermetallic layer was about 40.07, 58.62 and 97.34 µm at the same immersion times. We notice that the thickness is reduced to about one-third of that observed in hot dipping into the aluminum bath and this is explained by the addition of silicon in the aluminum melt which reduces strongly the thickness of the reaction zone. This result agrees with the work of EGGLER et al. [24] and Cheng et al. [25] who found that silicon has an inhibiting effect on the growth of the intermetallic layer at the interface steel/coating.

These observations indicate that the addition of Si in the Al melt reduces the growth rate of the intermetallic layer and influences the morphology too. Since then, it has been reported [13] that the addition of an element in the Al bath forms solid solutions or phases that reduce the diffusion rate of the iron or aluminum atoms across the intermetallic layer and then reduces the growth rate of the intermetallic layer.

The cross-sectional BSE micrograph of mild steel hot dipped in aluminum–silicon bath for 3 h is shown in Fig. 4, and the corresponding EDS analysis is given in Table 3.

As for the steel dipped in Al, the aluminide layers were composed of an outer Al–Si topcoat and an inner intermetallic layer. The intermetallic layer is composed of Fe_2Al_5 and $FeAl_3$ phases in addition to two Fe–Al–Si intermetallics. Al_8Fe_2Si layer is formed above $FeAl_3$, and $Fe_3Al_2Si_3$ is formed between $FeAl_3$ and Fe_2Al_5. In the Al–Si topcoat, we found scattered compounds which possess a polyhedral morphology and some plate-shaped particles. Also, the Al_8Fe_2Si phase was detected directly at the steel/coating interface toward the Al–Si alloy coating and possessed an irregular polygonal shape. The irregular shape results from the diffusion of iron into the liquid Al during the hot dipping leading to solidification of Al_8Fe_2Si at the steel/coating interface.

Figure 5b shows the EDS lines scan profile of Al, Fe and Si along the white arrow in Fig. 5a. The measurements are taken on steel dipped for 3 h in the Al–Si bath, starting from

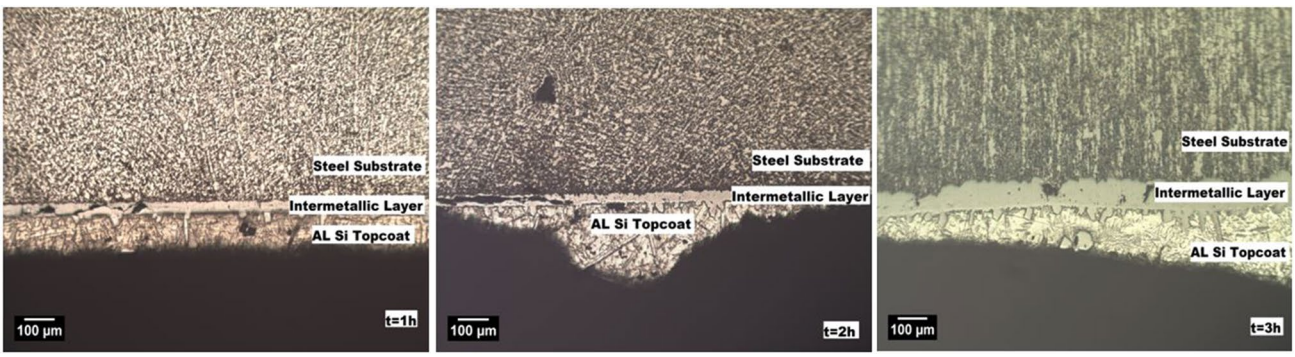

Fig. 3 Optical cross-sectional micrographs of mild steel after hot dipping into Al–Si bath at 750 °C at different immersion times ($t = 1$ h, 2 h and 3 h)

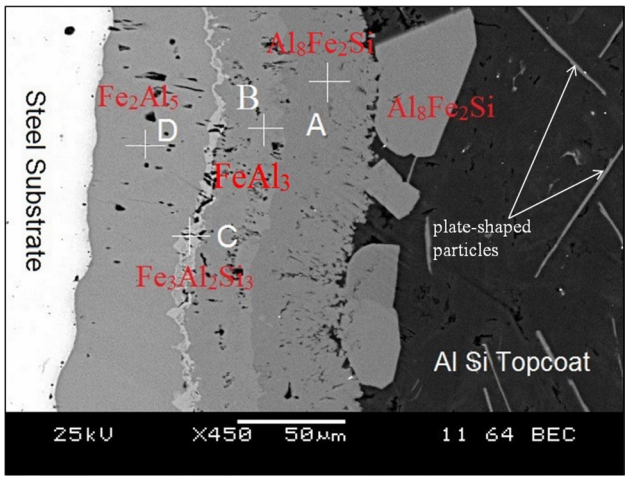

Fig. 4 Cross-sectional BSE micrograph of intermetallic layers in mild steel after hot dipping in Al–Si bath at 750 °C for 3 h

Table 3 The average composition of intermetallic phases in the aluminide layer on mild steel hot dipped into molten Al–Si for 3 h at 750 °C (at.%)

Position	Al K	Fe K	Si K	Phase
A	69.11	17.62	13.27	Al_8Fe_2Si
B	71.44	22.34	06.21	$FeAl_3$
C	40.38	33.48	26.15	$Fe_3Al_2Si_3$
D	69.54	27.79	02.67	Fe_2Al_5

the steel substrate to the aluminum–silicon topcoat. The concentration profile changes continuously across the intermetallic layer. The changing concentration of the elements suggests that the layer is composed of numerous phases. Al_8Fe_2Si phase is directly adjacent to the Al–Si coating followed by $FeAl_3$, and the profile shows a Si peak in the continuous white layer, at the interface between Fe_2Al_5 and $FeAl_3$ and corresponds to the $Fe_3Al_2Si_3$ phase.

In the XRD (Fig. 6), peaks of high intensity corresponding to the iron phase are detected. The other peaks correspond to Fe_2Al_5, $FeAl_3$, Al_8Fe_2Si and $Fe_3Al_2Si_3$ phases. We find peaks that were identified as $Fe_{4.5}AlSi$. This phase could correspond to the plate-shaped particles scattered in the Al–Si topcoat.

The interface between Fe_2Al_5 layer and steel substrate transformed from the tongue-like morphology into a flat morphology. This effect is attributed to the silicon present in the aluminum bath, which subsequently reduces the diffusivity of aluminum atoms in Fe_2Al_5 layer by occupying the vacancies in the c-axis of the crystal structure of Fe_2Al_5 [26].

The thickness of the Fe_2Al_5 phase is reduced from 570 µm in aluminizing with pure aluminum, to about 85 µm in aluminizing with Al–Si. This reducing in thickness may be explained by the formation of the ternary phase $Fe_3Al_2Si_3$, which could act as a diffusion barrier. The presence of ternary phases could influence the growth of the Fe_2Al_5 phase, either by its nucleation or by its role as a diffusion barrier. According to our results, the Si enrichments in the white band considered as the $Fe_3Al_2Si_3$ phase constitute a diffusion barrier for the Al atoms in the Al bath containing 10 wt.% Si, thereby reducing the growth of Fe_2Al_5 phase [27, 28]. $Fe_3Al_2Si_3$ phase observed at $FeAl_3/Fe_2Al_5$ interface possesses the highest iron content and high silicon content (about 33.48 at.% iron and 26.15 at.% silicon in this study), and the lower silicon content in the Fe_2Al_5 phase (2.67 at.%) shows that silicon is less soluble in the Fe_2Al_5 phase [29].

Studies concerning the formation of hexagonal Al_8Fe_2Si phase [30] have indicated that this phase is formed preferentially at a relatively slower solidification rate. As the silicon content in the aluminum bath increased and

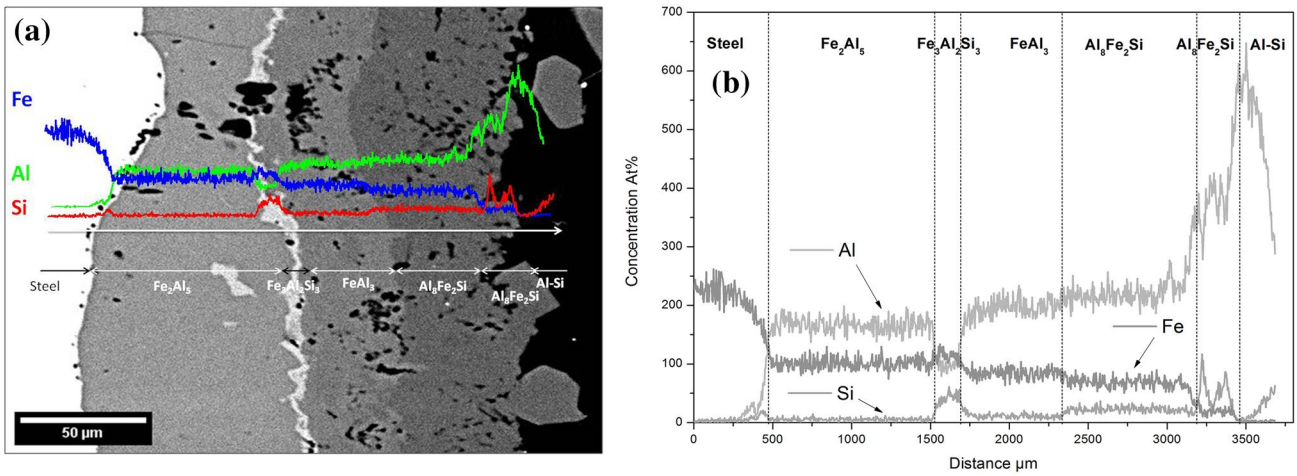

Fig. 5 EDS lines scan obtained on a specimen dipped for 3 h in Al–Si bath

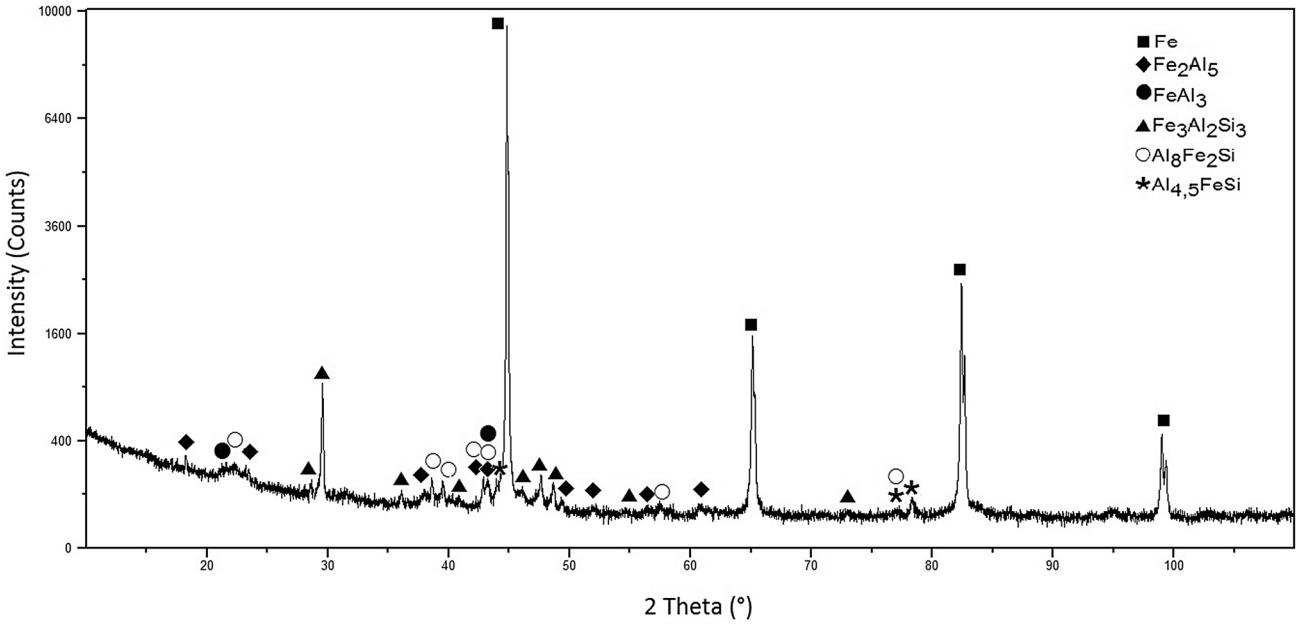

Fig. 6 XRD patterns of intermetallic layers formed in the hot-dip aluminized specimen in Al–Si at 750 °C for 3 h

approached the eutectic point of aluminum and silicon, the liquidus line of the molten aluminum bath decreased from 660 °C for pure aluminum to 600 °C for Al-13% Si. This decrease of the liquidus line of the Al–Si melt is because the Al–Si bath would possess a relatively slower solidification rate than a pure Al bath cooled from the temperature of 750 °C to room temperature. Consequently, in this study, the formation of hexagonal Al_8Fe_2Si is due to the solidification rate of residual aluminum–silicon liquid on the surface of the steel that was slowed down by adding 10 wt.% of silicon to the aluminum bath.

Microhardness Measurement

Figure 7 shows the microhardness measurements in the cross section of the steel hot dipped in Al and Al–Si bath at 750 °C for 3 h.

The intermetallic layer formed between Al and steel substrate has average microhardness values above $854Hv_{01}$ compared to the average microhardness of the aluminum coating layer of about $86.1Hv_{01}$ and that of the steel about $195Hv_{01}$, whereas in the Al–Si bath, the average microhardness values of the intermetallic layer are above $790Hv_{01}$. The fragility is therefore very marked, and when carrying out the

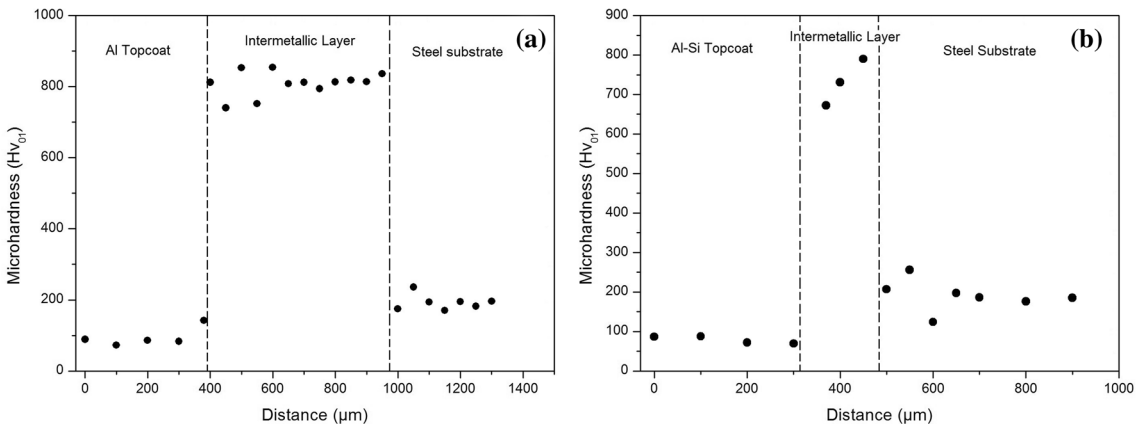

Fig. 7 Microhardness distributions from the coating to the steel substrate after hot dipping at 750 °C for 3 h in (**a**) Al bath, (**b**) Al–Si bath

test, the indentation causes cracks around the impression of microhardness.

$Al_xFe_ySi_z$ phases formed between steel and Al–Si coating have a lower microhardness compared with Fe_xAl_y phases in samples coated with Al and are more brittles.

The steel, whose initial hardness is about 246 Hv_{01}, undergoes a softening when immersed in liquid aluminum at 750 °C, resulting in a decrease in its hardness (values that vary between 236 Hv_{01} and 146 Hv_{01}). This decrease in microhardness is due to the annealing of steel. Indeed, the temperature of 750 °C, the holding time (3 h of immersion) and the relatively slow cooling (ambient air) represent the cycle of the annealed heat treatment.

In our case, in the absence of mechanical stress, the phenomenon of softening of the steel is of thermal origin. Indeed, the reactive environment, favoring the diffusion of iron and aluminum atoms, can be the origin of the fluctuations of the hardness of the steel at depth.

Conclusion

The formation of aluminide layers on mild steel during hot-dip aluminizing process at 750 °C was investigated. Two intermetallic phases have been identified in the pure aluminum bath, $FeAl_3$ phase near the aluminum topcoat and a major Fe_2Al_5 phase with tongue-/finger-like morphology oriented perpendicularly to the surface of the mild steel. The aluminide layer was thick and increases with increasing in dipping time. The presence of Si in Al melt influenced the overall thickness of the aluminide layers which seems to decrease, and the interface tends to become planar. Besides, it influences the growth of Fe_2Al_5 phase and resulted in the reduction of this layer. In addition to $FeAl_3$ and Fe_2Al_5 phases, two other phases Al_8Fe_2Si and $Fe_3Al_2Si_3$ were detected. Also, $Fe_{4.5}AlSi$ phase was found in the Al–Si topcoat and confirmed by XRD pattern. The very high values of microhardness Hv (above 800Hv_{01}) confirm the high brittleness of the intermetallic layer and allow to notice the softening by annealing of the steel after the process of hot-dip aluminizing.

The adherent coating of Al or Al–Si will offer good protection to the steel since the interest of this process is increasing the corrosion and oxidation resistance. For future work, it would be interesting to study the influence of intermetallic layers on the corrosion behavior of aluminized steel.

References

1. Y.N. Chang, F.I. Wei, High-temperature oxidation of low alloy steels. J. Mater. Sci. **24**, 14–22 (1989)
2. B. Schmid, N. Aas, Q. Grong, R. Qdegard, High-temperature oxidation of iron and the decay of wüstite studied with in situ ESEM. J. Oxid. Met. **57**, 116 (2002)
3. S. Kobayashi, T. Yakou, Control of intermetallic compound layers at interface between steel and aluminum by diffusion-treatment. J. Mater. Sci. Eng. A **338**, 44–53 (2002)
4. Y.Y. Chang, C.C. Tsaur, J.C. Rock, Microstructure studies of an aluminide coating on 9Cr-1Mo steel during high-temperature oxidation. J. Surf. Coat. Technol. **200**, 6588–6593 (2006)
5. C.J. Wang, S.M. Chen, The high-temperature oxidation behavior of hot-dipping Al-Si coating on low carbon steel. J. Surf. Coat. Technol. **200**, 6601–6605 (2006)
6. H. Glasbrenner, H.U. Borgstedt, Preparation and characterization of Al_20_3/Fe_xA1_y layers on MANET steel. J. Nucl. Mater. **212–215**, 1561–1565 (1994)
7. E. Serra, H. Glasbrenner, A. Perujo, Hot-dip aluminum deposit as a permeation barrier for MANET steel. J. Fusion. Eng. Des. **41**, 149–155 (1998)
8. Y. Kitajima, S. Hayashi, T. Nishimoto, T. Narita, S. Ukai, Rapid Formation of α-Al2O3 Scale on an Fe-Al Alloy by pure-metal coatings at 900°C. J. Oxid. Met. **73**, 375–388 (2010)
9. D. Wang, Z. Shi, Aluminizing and oxidation treatment of 1Cr18Ni9 stainless steel. J. Appl. Surf. Sci. **227**, 255–260 (2004)
10. W. Deqing, Phase evolution of an aluminized steel by oxidation treatment. J. Appl. Surf. Sci. **254**, 3026–3032 (2008)
11. W.J. Cheng, Y.Y. Chang, C.J. Wang, Observation of high-temperature phase transformation in the aluminide Cr–Mo steel using EBSD. J. Surf. Coat. Technol. **203**, 401–406 (2008)
12. R.W. Richards, R.D. Jones, P.D. Clements, H. Clarke, Metallurgy of continuous hot-dip aluminizing. J. Int. Mater. Rev. **39**, 191–212 (1994)
13. K. Bouché, F. Barbier, A. Coulet, Intermetallic compound layer growth between solid iron and molten aluminum. J. Mater. Sci. Eng. A **249**, 167–175 (1998)
14. A. Bahadur, O.N. Mohanty, Structural studies of hot-dip aluminized coatings on mild steel. J. Mater. Trans. JIM **32**, 1053–1061 (1991)
15. S. Mendil, K. Taibi, S. Azem, N. Harb, Growth of intermetallic phases during interdiffusion between steel and aluminum, in: *3ème Conférence Internationale sur le Soudage, le CND et l'Industrie des Matériaux et Alliages (IC-WNDT-MI'12)*, 26–28 Novembre 2012, Oran, Algerie
16. S. Mendil, S. Azem, K. Taibi, Identification of Fe-Al intermetallic phases in aluminide coatings on mild steel, in: *5th International Conference on Welding, Non-Destructive Testing and Materials and Alloys Industry (IC-WNDT-MI'16)*, November 26-28th, 2016, Oran, Algeria
17. I.I. Danzo, Y. Houbaert, K. Verbeken, Diffusion driven columnar grain growth induced in an Al-Si-coated steel substrate. J. Surf. Coat. Technol. **251**, 15–20 (2014)
18. W.J. Cheng, C.J. Wang, Effect of silicon on the formation of intermetallic phases in aluminide coating on mild steel. J. Intermet. **19**, 1455–1460 (2011)
19. F.M. Robert, *Metals handbook*, vol. 5 (American Society of Metals, Materials Park, 1983)
20. W.J. Cheng, C.J. Wang, Growth of intermetallic layer in the aluminide mild steel during hot-dipping. J. Surf. Coat. Technol. **204**, 824–828 (2009)
21. U.R. Kattner, B.P. Burton, *Phase Diagrams of Binary Iron Alloys* (ASM International, Materials Park, Ohio, 1993)
22. G. Haiyan, H. Yuehui, S. Peizhi, Z. Jin, X. Nanping, J. Yao, H. Baiyun, C.T. Liu, Porous FeAl intermetallics fabricated by elemental powder reactive synthesis. J. Intermet. **17**, 1041–1046 (2009)
23. T. Maitra, S.P. Gupta, Intermetallic compound formation in Fe-Al-Si ternary system. J. Mater. Charact. **49**, 293–311 (2003)

24. G. Eggeler, W. Auer, H. Kaesche, On the influence of silicon on the growth of the alloy layer during hot-dip aluminizing. J. Mater. Sci. **21**, 3348–3350 (1986)
25. W.J. Cheng, C.J. Wang, Microstructural evolution of intermetallic layer in hot-dipped aluminide mild steel with silicon addition. J. Surf. Coat. Technol. **205**, 4726–4731 (2011)
26. T. Heumann, S. Dittrich, Über die Kinetik der Reaktion von festem und flüssigem Aluminium mit Eisen. J. Z Metallkd. **50**, 617–625 (1959)
27. B. Lemmens, H. Springer, M.J. Duarte, I. De Graeve, J. De Strycker, D. Raabe, K. Verbeken, Atom probe tomography of intermetallic phases and interfaces formed in dissimilar joining between Al alloys and steel. J. Mater. Charact. **120**, 268–272 (2016)
28. B. Lemmens, H. Springer, I. De Graeve, J. De Strycker, D. Raabe, K. Verbeken, Effect of silicon on the microstructure and growth kinetics of intermetallic phases formed during hot-dip aluminizing of ferritic steel. J. Surf. Coat. Technol. **319**, 104–109 (2017)
29. F. Bosselet, D. Pontevichi, M. Sacerdote-Peronnet, J.C. Viala, Measurement of the isothermal section at 1000 K of Al-Fe-Si. J. Phys IV France **122**, 41–46 (2004)
30. H. Tanihata, T. Sugawara, K. Matsuda, S. Ikeno, Effect of casting and homogenizing treatment conditions on the formation of Al-Fe-Si intermetallic compounds in 6063 Al-Mg-Si alloys. J. Mater. Sci. **34**, 1205–1210 (1999)